

1 Neutralization of SARS-CoV-2 variants by convalescent and 2 vaccinated serum

3

4 Timothy A. Bates^{1*}, Hans C. Leier^{1*}, Zoe L. Lyski¹, Savannah K. McBride¹, Felicity J.
5 Coulter¹, Jules B. Weinstein¹, James R. Goodman², Zhengchun Lu¹, Sarah A. R. Siegel
6 ³, Peter Sullivan³, Matt Strnad³, Amanda E. Brunton³, David X. Lee¹, Marcel E.
7 Curlin^{4,#}, William B. Messer^{1,3,4,#}, Fikadu G. Tafesse^{1,#}

8

9 Affiliations

10 ¹Department of Molecular Microbiology & Immunology, Oregon Health & Science
11 University (OHSU), Portland, OR 97239, USA.

12 ²Medical Scientist Training Program, Oregon Health & Science University (OHSU),
13 Portland, OR 97239, USA

14 ³OHSU-PSU School of Public Health, Program in Epidemiology, Portland, OR 97339,

15 ⁴USA Department of Medicine, Division of Infectious Diseases, Oregon Health &
16 Science University (OHSU), Portland, OR 97239, USA.

17 *these authors contributed equally to this work.

18

19

20

21

22 #Correspondence to: Fikadu G. Tafesse tafesse@ohsu.edu, William B. Messer

23 messer@ohsu.edu, Marcel E. Curlin, curlin@ohsu.edu

24

25 **Abstract**

26 We tested human sera from large, demographically balanced cohorts of BNT162b2
27 vaccine recipients (n=51) and COVID-19 patients (n=44) for neutralizing antibodies
28 against SARS-CoV-2 variants B.1.1.7 and B.1.351. Although the effect is more
29 pronounced in the vaccine cohort, both B.1.1.7 and B.1.351 show significantly reduced
30 levels of neutralization by vaccinated and convalescent sera. Age is negatively
31 correlated with neutralization in vaccinee, and levels of variant-specific RBD antibodies
32 are proportional to neutralizing activities.

33

34

35

36

37

38

39

40

41

42

43

44

45

46

47 **Main**

48 Since its emergence in Wuhan, China in late 2019, severe acute respiratory syndrome
49 coronavirus 2 (SARS-CoV-2) has spread worldwide, causing widespread illness and
50 mortality from coronavirus 2019 disease (COVID-19).¹ Continued SARS-CoV-2
51 transmission has led to the emergence of variants of concern (VOCs) that show
52 evidence of increased transmissibility or resistance to prior immunity.² By early 2021,
53 three major VOCs were widely recognized: B.1.1.7, first identified in southeast England
54 in November 2020³; B.1.351, identified in November in South Africa; and P.1, identified
55 in December Brazil^{3,4}. These VOCs were associated with increases in infections and
56 hospitalizations in their countries of origin, and all have increased in frequency in other
57 regions, suggesting a competitive fitness advantage over existing lineages.⁵

58 Though a relatively small number of nonsynonymous mutations and deletions
59 distinguish VOCs from earlier lineages (Supplementary Table 1), many of these encode
60 residues in the spike protein, which interacts with the SARS-CoV-2 cellular receptor,
61 angiotensin-converting enzyme 2 (ACE2), via its receptor-binding domain (RBD)^{6,7}.
62 RBD mutations could potentially increase transmissibility by enhancing binding to
63 ACE2, or promote immune escape by altering epitopes that are the primary target of
64 potentially neutralizing antibodies.⁷ In fact, the most prominent mutation that appeared
65 early in the pandemic and rose to near-fixation in new strains was a substitution at spike
66 residue position 614 (D614G) which positions the RBD in a more accessible
67 configuration and confers greater infectivity but also greater susceptibility to neutralizing
68 antibodies.^{8,9}

69 In addition to sharing D614G and a N501Y substitution which is associated with
70 greater ACE2 affinity,¹⁰ VOCs have acquired other spike mutations, some of which are
71 associated with resistance to antibody neutralization. These include E484K and
72 K417N/T, both of which arose independently in the B.1.351 and P.1 lineages.¹¹⁻¹³
73 Epidemiological reports suggest that natural immunity to earlier SARS-CoV-2 lineages
74 may confer limited protection from reinfection by B.1.351 or P.1^{3,14}, and prior analyses
75 using relatively small numbers of vaccinee sera against pseudotyped or chimeric
76 viruses showed reduced neutralization of B.1.351 and P.1^{13,15}. The purpose of this
77 study was to use neutralization assays with clinical virus isolates to rigorously examine
78 the potency of antibodies elicited by the BNT162b2 vaccine or natural infection against
79 the broader antigenic RBD variability within the B.1.1.7 and B.1.351 variants.

80 The three COVID-19 vaccines authorized for emergency use by the U.S. Food
81 and Drug Administration (BNT162b2 [Pfizer–BioNTech], mRNA-1273 [Moderna], and
82 Ad26.COV2.S [Janssen]) elicit immunity using a spike protein antigen derived from
83 early isolates such as USA_WA1/2020 (WA1)¹⁶. RBD-binding antibody levels in adults
84 who had received two doses of the BNT162b2 mRNA vaccine were determined by
85 ELISA using recombinant RBD from WA1 (RBD-WA1) and RBDs with substitutions
86 possessed by B.1.1.7 (N501Y) and B.1.351 (N501Y, E484K, K417N) (Table S1).
87 Compared to that of RBD-WA1, vaccinated patient sera had a geometric mean 50%
88 effective concentration (EC50) which was 1.3-fold lower (P=0.0411) for RBD-B.1.1.7
89 and 1.4-fold lower (P=0.0047) for RBD-B.1.351 (Figure 1A). BNT162b2-elicited
90 antibodies also displayed potent neutralizing activity against WA1 in a 50% focus
91 reduction neutralization tests (FRNT50) (geometric mean titer (GMT) 1:393 +/- 2.5) but

92 decreased neutralization of B.1.1.7 (GMT 1:149 +/- 2.4) and B.1.351 (GMT 1:45 +/-
93 2.3), representing 2.6-fold ($P < 0.0001$) and 8.8-fold ($P < 0.0001$) reductions, respectively
94 (Figures 1B and S1). The positive correlation between serum EC50 and NT50 was
95 consistent for each matched variant-RBD pair, indicating that variant-specific RBD-
96 targeted antibody concentration is proportional to live virus neutralization capacity
97 against each lineage (Figure 1C).

98 There was individual variation in the relative neutralization of the different
99 variants. Neutralizing titers for WA1 and B.1.1.7 were highly correlated at the individual
100 level (Figure 1D). In contrast, WA1 and B.1.351 FRNT50 titers correlated weakly at the
101 individual level, with some individual's serum potentially neutralizing WA1 while having
102 FRNT50 for B.1.351 below the assay limit of detection (1:20) (Figure 1E).

103 Older adults make up the most vulnerable population to COVID-19 and therefore
104 have been prioritized for vaccination¹⁹. We found similar age-dependent decline in
105 FRNT50 titers against each lineage in our study (Figures 1F-H). These differences were
106 highly significant for all three variants between subgroups of younger (20-50 y.o. n=25)
107 and older (>50 y.o. n=25) adults in our cohort (Figure 1I). There was no correlation
108 between gender and neutralization titers after vaccination.

109 In contrast to the spike-specific antibody repertoire raised by BNT162b2
110 vaccination, the antibody response to SARS-CoV-2 infection is more antigenically
111 diverse⁷. Overall, RBD binding activities against all lineages were significantly lower in
112 convalescent sera compared to vaccinee sera across all sample timepoints (1-301 days
113 post-PCR positive) (Figures 1A and 2A and 2B). Moreover, there was no observable
114 difference in convalescent serum EC50 between RBD-WA1, RBD-B.1.1.7, and RBD-

115 B.1.351 (Figure 2B). In convalescent sera, there was also no clear correlation between
116 variant-specific RBD binding and neutralization (Figure 2C). To better capture the
117 reduced antibody levels, we modified our ELISA protocol to reduce the limit of detection
118 to 1:200 (compared with 1:1600 for vaccinee ELISAs). Differences in FRNT50 titer
119 against WA1 and the VOCs were similarly reduced overall compared to vaccinee sera
120 (WA1, GMTs 1:52.1 +/- 4.3; B.1.1.7, 1:36.8 +/- 3.0; B.1.351, 28.8 +/- 2.3) but showed
121 substantially less variability with a 1.8-fold drop (CI) for B.1.351 and a 1.4-fold drop (CI)
122 for B.1.1.7 relative to WA1 (Figures 2C and S2). Many convalescent sera fell below the
123 FRNT limit of detection (Figures 2D-E): for WA1, 43% of convalescent cohort sera failed
124 to neutralize $\geq 50\%$ of input virus at the lowest dilution, and this proportion was even
125 greater for the VOCs (B.1.1.7, 54%; B.1.351, 64%).

126 An important question surrounding the increasing evidence of reinfection in
127 convalescent individuals by VOC is whether the severity of disease during the initial
128 exposure is related to protection, or lack thereof, from reinfection³. Neutralizing titer in
129 the convalescent cohort showed no significant correlation with the time between first
130 confirmatory positive PCR result and sample collection, indicating relatively stable
131 FRNT50 values over timescales up to 301 days (Figure 2F). Additionally, no correlation
132 was found between neutralizing titer for any lineage and patient age, sex, or
133 hospitalization for COVID-19 (Figures S3 and S4).

134 In this study we provide evidence of reduced antibody-mediated immunity to
135 newly emerging SARS-CoV-2 variants B.1.1.7 and B.1.351 after immunization with the
136 Pfizer-BioNTech COVID-19 vaccine or following natural infection. Our study involves a
137 relatively large cohort, provides data well-balanced for gender and age distribution,

138 controls for time since vaccination, and directly compares early-type and two newly
139 emerging SARS-CoV-2 variants of global concern. Critically, we use authentic clinical
140 isolates that display the native antigenic landscape of the virus, an approach that
141 provides the best possible examination of antibody activity against these viruses.

142 While it is likely that the resistance of some VOCs to neutralization is driven by
143 accumulated mutations in the RBD and the rest of the spike protein, and there is
144 evidence that high levels of RBD-binding antibodies is a meaningful correlate of
145 protection from isogenic lineages^{7,17}, other features of host immunity may contribute to
146 protection. Specifically, the neutralization titers seen in our convalescent subjects, while
147 lower overall, have a smaller gap in neutralizing activity between WA1 and VOCs than
148 in BNT162b2 vaccinees. This difference between convalescents and vaccinees
149 suggests that SARS-CoV-2 infection may elicit more broadly cross-reactive and
150 potentially cross-neutralizing antibodies, even with reduced affinity for mutant RBDs.
151 This notion has a strong foundation in coronavirus research, as there is substantial
152 cross-reactivity of anti-SARS-CoV spike antibodies with SARS-CoV-2 spike¹⁸. Indeed,
153 risk of reinfection by VOCs may be driven by generally low serological responses in
154 most COVID-19 patients, rather than the presence of RBD mutations that allow immune
155 escape. Other arms of the adaptive immune response that we did not explore here,
156 such as T cell immunity, could also contribute to cross-lineage immunity¹⁹.

157 A particularly significant finding was the negative correlation between age and
158 neutralizing antibody titer against VOCs in vaccinees, given that age is the predominant
159 risk factor for severe COVID-19²⁰ and patients of advanced age stand to benefit the
160 most from vaccination. Longitudinal studies of this and other cohorts could examine the

161 durability of vaccine-induced immune responses, and should be designed to resolve the
162 nature of antibody responses induced by vaccination or natural infection that may
163 correlate with broad cross-neutralization. This will be particularly important for
164 developing vaccines that will be effective in vulnerable populations, including those of
165 advanced age, against future SARS CoV-2 variants.

166

167 **Acknowledgements**

168 The authors thank the generous contribution of the many patients and vaccinees who
169 participated in this study. In addition, we gratefully acknowledge the efforts of the entire
170 OHSU Covid-19 serology study team.

171

172 **Funding**

173 This study was funded in part by an unrestricted grant from the M.J. Murdock Charitable
174 Trust, by NIH training grant T32AI747225 on Interactions at the Microbe-Host Interface,
175 and OHSU Innovative IDEA grant 1018784, and NIH R01AI145835.

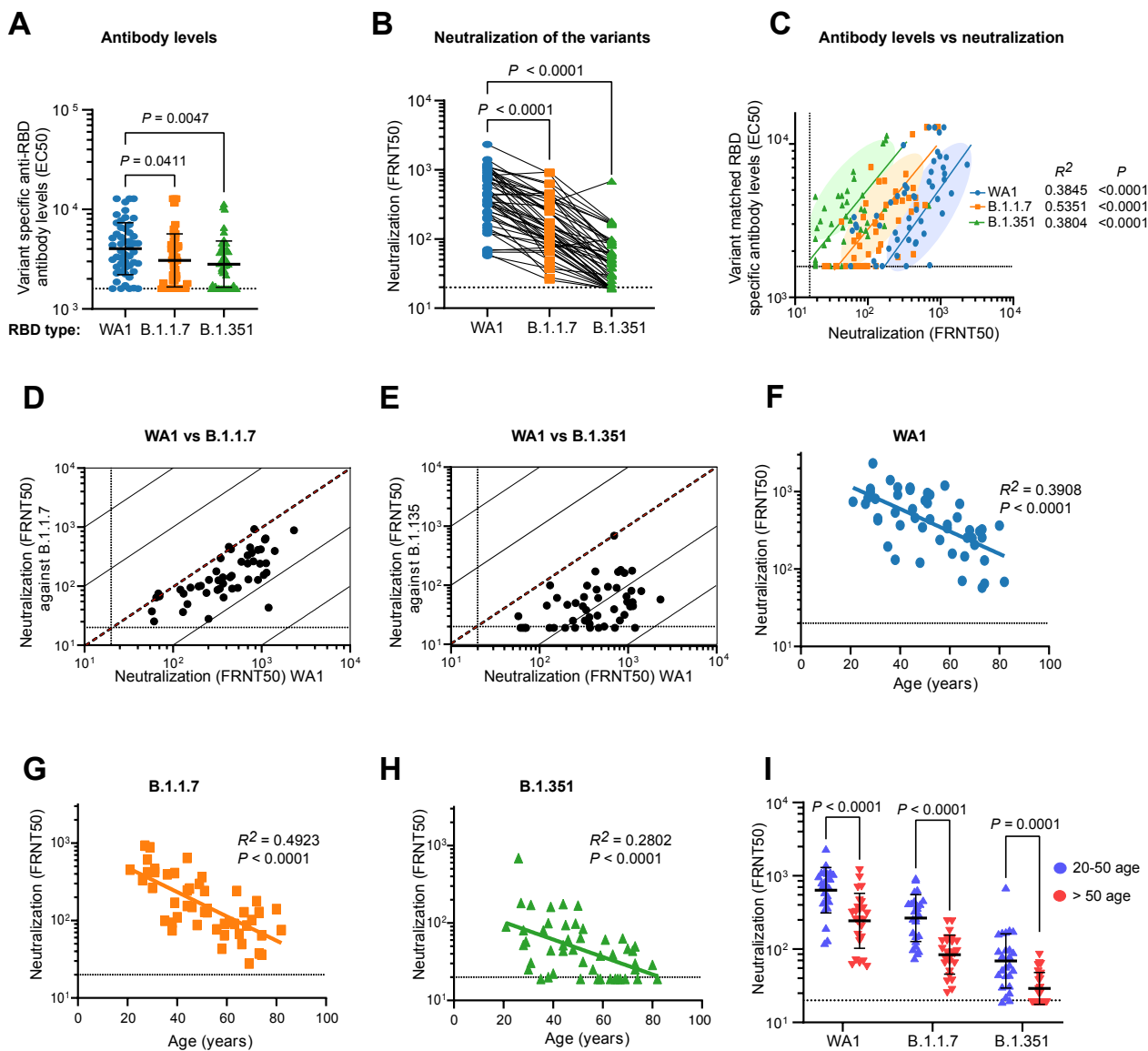
176

177

Table 1. Demographic characteristics of study participants			
Convalescent serum donors			
Characteristic	Hospitalized		Total (N=54)
	Yes (n=17)	No (n=37)	
Median age – yr (range)	56 (22-88)	54 (1-80)	56 (1-88)
Sex – no. (%)			
Female	11 (35.4)	20 (64.5)	31 (57.4)
Male	6 (26.1)	17 (73.9)	23 (42.6)
Symptomatic – no. (%)			
No	3 (17.6)	1 (2.70)	4 (7.40)
Yes	14 (82.4)	36 (97.3)	50 (92.6)
Admitted to ICU – no. (%)			
Yes	5 (29.4)	NA	5 (9.25)
No	12 (70.6)	NA	12 (22.2)
Median time between first positive COVID-19 PCR test and sample collection – days (range)	21 (1-217)	197 (22-302)	188.5 (1-302)
BNT162b2-vaccinated donors			
Characteristic	Total (N=51)		
Median age – yr (range)	50 (21-82)		
Sex – no. (%)			
Female	28 (54.9)		
Male	23 (45.1)		
Median time between vaccine doses – days (range)	21 (20-22)		
Median time between second dose and sample collection – days (range)	14 (14-15)		

178

BNT162b2 vaccine

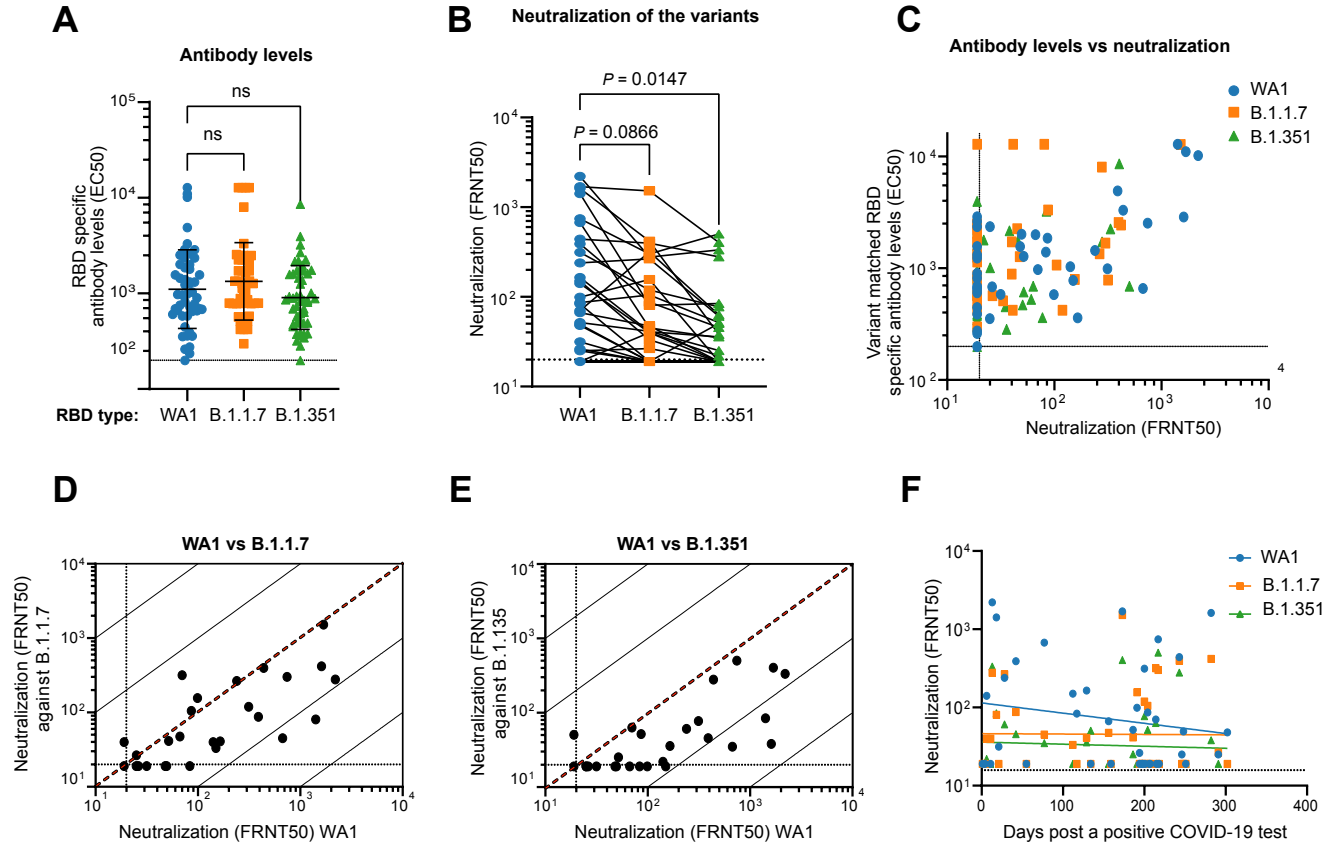


179

180 **Figure 1. Serum antibody levels of BNT162b2 vaccine recipients and potency of sera to**
 181 **neutralize SARS-CoV-2 variants.** A) Serum antibody levels (EC50) that recognize the spike
 182 RBD of the wild type USA-WA1/2020 (WA1), B.1.1.7, and B.1.351 variants are shown. The
 183 RBD-B.1.1.7 carries the N501Y mutation corresponding to the B.1.1.7 variant and the RBD-
 184 B.1.135 has K417N, E484K, and N501Y mutations that are present in the B.1.351 variant. B)
 185 Comparison of neutralization titers (FRNT50) between WA1, B.1.17 and B.1.351 for BNT162b2
 186 vaccinee sera. C) Correlation of variant matched RBD-specific antibody levels and
 187 neutralization titers (FRNT50) of the AW1 virus and the two variants. D, E) Correlations between
 188 neutralization titers of the B.1.1.7 (D) and B.1.351 (E) variants with the WA1 virus. The dotted
 189 diagonal lines indicate identical neutralization, and the solid diagonal black lines indicate 10-fold
 190 differences in neutralization. F-H) Correlation between participant age and neutralization titer
 191 against WA1 (F), B.1.1.7 (G), and B.1.351 (H). I) Effect of age range on the neutralization
 192 potency among the BNT162b2 vaccine recipients.

193
194

Natural infection



195
196
197
198
199
200
201
202
203
204
205
206
207
208
209
210
211
212
213
214

Figure 2. Neutralization of SARS-CoV-2 variants by convalescent serum.

A) Quantification of serum antibody levels (EC50) that recognize RBD protein corresponding to the wild type (WA1), B.1.1.7, and B.1.351 variants. B) Comparison of neutralization titers between WA1, B.1.17 and B.1.351 for convalescent sera. C) Relationship between convalescent antibody levels and neutralization (FRNT50) of the different virus strains. D, E) Correlations between convalescent serum neutralization titer of the B.1.1.7 (D) and B.1.351 (E) variants with the WA1 virus. The dotted diagonal lines indicate identical neutralization, and the solid diagonal black lines indicate 10-fold differences in neutralization. F) Correlation of convalescent neutralization titers with time after first positive PCR test in COVID-19 patients. There is no significant correlation between days post positive PCR test and FRNT50 for the viral strains tested.

215 References

- 216
- 217 1 Noh, J. & Danuser, G. Estimation of the fraction of COVID-19 infected people in U.S.
218 states and countries worldwide. *PLoS One* **16**, e0246772,
219 doi:[10.1371/journal.pone.0246772](https://doi.org/10.1371/journal.pone.0246772) (2021).
- 220 2 Plante, J. A. *et al.* The Variant Gambit: COVID's Next Move. *Cell Host Microbe*,
221 doi:<https://doi.org/10.1016/j.chom.2021.02.020> (2021).
- 222 3 Sabino, E. C. *et al.* Resurgence of COVID-19 in Manaus, Brazil, despite high
223 seroprevalence. *Lancet* **397**, 452-455, doi:[10.1016/S0140-6736\(21\)00183-5](https://doi.org/10.1016/S0140-6736(21)00183-5) (2021).
- 224 4 Tegally, H. *et al.* Emergence and rapid spread of a new severe acute respiratory
225 syndrome-related coronavirus 2 (SARS-CoV-2) lineage with multiple spike mutations in
226 South Africa. *medRxiv*, 2020.2012.2021.20248640, doi:[10.1101/2020.12.21.20248640](https://doi.org/10.1101/2020.12.21.20248640)
227 (2020).
- 228 5 Walensky, R. P., Walke, H. T. & Fauci, A. S. SARS-CoV-2 Variants of Concern in the United
229 States-Challenges and Opportunities. *JAMA*, doi:[10.1001/jama.2021.2294](https://doi.org/10.1001/jama.2021.2294) (2021).
- 230 6 Lan, J. *et al.* Structure of the SARS-CoV-2 spike receptor-binding domain bound to the
231 ACE2 receptor. *Nature* **581**, 215-220, doi:[10.1038/s41586-020-2180-5](https://doi.org/10.1038/s41586-020-2180-5) (2020).
- 232 7 Robbiani, D. F. *et al.* Convergent antibody responses to SARS-CoV-2 in convalescent
233 individuals. *Nature* **584**, 437-442, doi:[10.1038/s41586-020-2456-9](https://doi.org/10.1038/s41586-020-2456-9) (2020).
- 234 8 Gobeil, S. M. *et al.* D614G Mutation Alters SARS-CoV-2 Spike Conformation and
235 Enhances Protease Cleavage at the S1/S2 Junction. *Cell Reports* **34**, 108630,
236 doi:[10.1016/j.celrep.2020.108630](https://doi.org/10.1016/j.celrep.2020.108630) (2021).
- 237 9 Plante, J. A. *et al.* Spike mutation D614G alters SARS-CoV-2 fitness. *Nature*,
238 doi:[10.1038/s41586-020-2895-3](https://doi.org/10.1038/s41586-020-2895-3) (2020).
- 239 10 Tian, F. *et al.* Mutation N501Y in RBD of Spike Protein Strengthens the Interaction
240 between COVID-19 and its Receptor ACE2. *bioRxiv*, 2021.2002.2014.431117,
241 doi:[10.1101/2021.02.14.431117](https://doi.org/10.1101/2021.02.14.431117) (2021).
- 242 11 Greaney, A. J. *et al.* Comprehensive mapping of mutations in the SARS-CoV-2 receptor-
243 binding domain that affect recognition by polyclonal human plasma antibodies. *Cell Host*
244 *Microbe*, doi:[10.1016/j.chom.2021.02.003](https://doi.org/10.1016/j.chom.2021.02.003) (2021).
- 245 12 Weisblum, Y. *et al.* Escape from neutralizing antibodies by SARS-CoV-2 spike protein
246 variants. *eLife* **9**, e61312, doi:[10.7554/eLife.61312](https://doi.org/10.7554/eLife.61312) (2020).
- 247 13 Garcia-Beltran, W. F. *et al.* Circulating SARS-CoV-2 variants escape neutralization by
248 vaccine-induced humoral immunity. *medRxiv*, 2021.2002.2014.21251704,
249 doi:[10.1101/2021.02.14.21251704](https://doi.org/10.1101/2021.02.14.21251704) (2021).
- 250 14 Novavax. (2021).
- 251 15 Xie, X. *et al.* Neutralization of SARS-CoV-2 spike 69/70 deletion, E484K and N501Y
252 variants by BNT162b2 vaccine-elicited sera. *Nature Medicine*, doi:[10.1038/s41591-021-](https://doi.org/10.1038/s41591-021-01270-4)
253 [01270-4](https://doi.org/10.1038/s41591-021-01270-4) (2021).
- 254 16 Forni, G. & Mantovani, A. COVID-19 vaccines: where we stand and challenges ahead.
255 *Cell Death & Differentiation* **28**, 626-639, doi:[10.1038/s41418-020-00720-9](https://doi.org/10.1038/s41418-020-00720-9) (2021).
- 256 17 Barnes, C. O. *et al.* SARS-CoV-2 neutralizing antibody structures inform therapeutic
257 strategies. *Nature* **588**, 682-687, doi:[10.1038/s41586-020-2852-1](https://doi.org/10.1038/s41586-020-2852-1) (2020).

- 258 18 Bates, T. A. *et al.* Cross-reactivity of SARS-CoV structural protein antibodies against
259 SARS-CoV-2. *Cell Reports*, 108737, doi:10.1016/j.celrep.2021.108737 (2021).
- 260 19 Zuo, J. *et al.* Robust SARS-CoV-2-specific T cell immunity is maintained at 6 months
261 following primary infection. *Nature Immunology*, doi:10.1038/s41590-021-00902-8
262 (2021).
- 263 20 Rosenthal, N., Cao, Z., Gundrum, J., Sianis, J. & Safo, S. Risk Factors Associated With In-
264 Hospital Mortality in a US National Sample of Patients With COVID-19. *JAMA Netw Open*
265 **3**, e2029058, doi:10.1001/jamanetworkopen.2020.29058 (2020).
266
267

268 **SUPPLEMENTARY INFORMATION**

269

270 **MATERIALS AND METHODS**

271

272 This study was conducted in accordance with the Oregon Health & Science University

273 Institutional Review Board (IRB#00022511 & #21230).

274

275 **Serum collection (Vaccinated cohort - IRB#00022511)**

276 Subjects were enrolled at Oregon Health & Science University immediately after receiving their

277 first dose of the Pfizer-BioNTech COVID-19 vaccine. After obtaining informed consent, 4-6 mL

278 of whole blood were collected (BD Vacutainer® Plus Plastic Serum Tubes) and centrifuged for

279 10 minutes at 1000 x g. A second blood sample was obtained 14-15 days after subjects received

280 their second dose of the Pfizer-BioNTech COVID-19 vaccine. Samples were stored at -20°C

281 until sera were collected for neutralization assay. A subset of serological samples (n=51) was

282 randomly selected while maintaining equal gender representation, balanced age distribution, time

283 between vaccination doses equal to 21 days +/- 1 day, and time from boost to blood sampling

284 equal to 14 days +/- 1 day. Randomization was performed using R version 4.0.3 in RStudio

285 version 1.2.5001.

286

287 **Serum collection (Natural infection cohort - IRB#21230)**

288 Subjects with confirmed COVID-19 infection were part of a larger cohort of COVID-19

289 individuals at the Oregon Health & Science University. After obtaining informed consent, 10mL

290 of whole blood was collected for serum (BD Vacutainer® Red Top Serum Tubes), and 40mL of
291 whole blood were collected for PBMCs and plasma (BD Vacutainer® Lavender Top EDTA
292 Tubes). Serum tubes were centrifuged for 10 minutes at 1000 x g. Samples were heat-inactivated
293 for 30 minutes at 56°C and stored at -20°C until needed. A subset of serological samples (n=54)
294 from individuals with time post infection (determined by date of first positive PCR) ranging from
295 1 day – 10 months, a spectrum of disease severity scores and clinical disease ranging from
296 asymptomatic to severe (hospitalized in the ICU) were chosen for this analysis.

297

298 **Cell culture**

299 Vero E6 monkey kidney epithelial cells (CRL-1586) were obtained from the ATCC. Unless
300 otherwise stated, cells were maintained at all times in standard tissue culture-treated vessels in
301 complete media (DMEM, 10% FBS, 1% nonessential amino acids, 1% penicillin-streptomycin)
302 at 37°C and 5% CO₂.

303

304 **SARS-CoV-2 growth and titration**

305 SARS-CoV-2 isolates USA/CA_CDC_5574/2020 [lineage B.1.1.7] (NR-54011), hCoV-19/South
306 Africa/KRISP-K005325/2020 [lineage B.1.351] (NR-54009), and USA-WA1/2020¹ [lineage A]
307 (NR-52281) were obtained through BEI Resources. Sub-confluent monolayers of Vero E6 cells
308 in 75 cm² flasks were inoculated with the p0 isolates and grown for 72 h, at which time
309 significant cytopathic effect was observed for all strains. Culture supernatants were removed,
310 centrifuged 10 min at 1,000 x g, and stored in aliquots at -80°C. To determine titer, confluent
311 monolayers of Vero E6 cells in 96-well plates were inoculated with tenfold serial dilutions of
312 SARS-CoV-2 prepared in dilution media (Opti-MEM, 2% FBS) for 1 h at 37°C, then covered

313 with overlay media (Opti-MEM, 2% FBS, 1% methylcellulose) and cultured an additional 24 h.
314 Overlay media was then removed, and plates were fixed for 1 h in 4% paraformaldehyde in PBS.
315 Foci were developed as described.² In brief, cells were permeabilized for 30 minutes in perm
316 buffer (0.1% BSA, 0.1% Saponin in PBS) and incubated with 1:5,000 anti-SARS-CoV-2 alpaca
317 serum for 2 hours at room temperature. Plates were washed three times with wash buffer (0.01%
318 Tween-20 in PBS), then incubated with 1:20,000 anti-alpaca-HRP (Novus #NB7242) for 2 hours
319 at room temperature. Plates were again washed three times with wash buffer and 30 μ L of KPL
320 TrueBlue substrate (Seracare #5510-0030) added to each well. Plates were incubated at room
321 temperature for 20 minutes and imaged with a CTL Immunospot Analyzer, then foci were
322 counted using CTL ImmunoSpot (7.0.26.0) Professional DC.

323

324 Additional SARS-CoV-2 isolates were propagated and titrated during the development of this
325 assay. They included the three previously described clinical isolates: USA/CA_CDC_5574/2020
326 [lineage B.1.1.7] (NR-54011), hCoV-19/South Africa/KRISP-K005325/2020 [lineage B.1.351]
327 (NR-54009), and USA-WA1/2020¹ [lineage A] (NR-52281) as well as two additional clinical
328 isolates: hCoV-19/South Africa/KRISP-EC-K005321/2020 [lineage B.1.351] (NR-54008) and
329 hCoV-19/England/204820464/2020 (NR-54000). Substantial differences were noted in the focus
330 phenotypes of these strains (Fig. S5).

331

332 **SARS-CoV-2 FRNT**

333 Serial dilutions of patient sera and virus neutralization were carried out in duplicate, using
334 separately prepared dilutions, in a 96-well plate format. Briefly, each sample was added in
335 duplicate 1:10 to dilution media, and 4 four-fold serial dilutions were made spanning a range

336 from 1:10 to 1:2560. An equal volume of dilution media containing 50 FFU of SARS-CoV-2
337 was added to each well (final dilutions of sera, 1:20 – 1:5120) and incubated 1 h at 37°C. The
338 virus-sera mixtures were then added to monolayers of Vero E6 in corresponding 96-well plates,
339 incubated 1 h at 37°C, and covered with overlay media. Fixation, foci development, and
340 counting were carried out as described above. Focus counts were used to calculate percent
341 neutralization by dividing by the average of positive control wells without patient serum
342 treatment.

343

344 **Production of variant RBDs**

345 Site-directed mutagenesis was used to introduce mutations into WT RBD. Purified SARS-CoV-2
346 WA1, B.1.1.7, and B.1.351 RBD protein was prepared as previously described.² Briefly,
347 sequence confirmed recombinant RBD lentiviruses was produced and used to generate stable
348 HEK293F cells, which were allowed to grow for 3 days before collecting the cell media and
349 purifying by Ni-NTA chromatography. The purified protein was buffer exchanged into PBS and
350 concentrated by 10 kDa cutoff column and purity was assessed by SDS-PAGE.

351

352 **ELISA**

353 ELISAs were performed in biological duplicate 96-well plates (Nunc™ MaxiSorp™ #423501).
354 Plates were coated 100 uL/well with purified wild-type SARS-CoV-2 RBD, RBD-501, or RBD-
355 3M constructs at 1 ug/mL in PBS and incubated overnight at 4°C with rocking. Plates were then
356 washed three times with wash buffer (0.05% Tween-20 in PBS) and blocked with 150 uL/well
357 blocking buffer (5% nonfat dry milk powder and 0.05% Tween-20 in PBS) at RT for 1 hour with
358 rocking. Infected and vaccinated patient sera were initially diluted in Opti-MEM in the 96-well

359 plate format used above. For the ELISA, diluted vaccinated and infected patient sera was further
360 diluted in blocking buffer on the plate (4×4-fold dilutions from 1:200 for infected patients; 4 2-
361 fold dilutions from 1:1,600 for vaccinated patients). After incubating at RT for 1 hour with
362 rocking, plates were washed three times. The secondary antibody Goat anti-Human IgG, IgM,
363 IgA (H+L) (Invitrogen, #A18847) was diluted in blocking buffer (1:10,000) and applied to the
364 plates 100 uL/well. Plates were protected from light and incubated at RT for 1 hour with rocking,
365 then washed three times prior to the addition of the peroxidase activity detector 3,3',5,5'-
366 tetramethylbenzidine (TMB, Thermo Scientific Pierce 1-Step Ultra TMB ELISA Substrate
367 #34029). The reaction was stopped after 5 minutes using an equivalent volume of 1 M H₂SO₄;
368 optical density (OD) was measured at 450 nm using a CLARIOstar plate reader. OD₄₅₀ readings
369 were normalized by subtracting the average of negative control wells and finally dividing by the
370 average maximum signal (95th percentile) for each unique coating protein in each experiment.

371

372 **FRNT50 and EC50 calculation**

373 Percent neutralization values for FRNT50 or normalized OD₄₅₀ values for EC₅₀ were compiled
374 and analyzed using python (v3.7.6) with numpy (v1.18.1), scipy (v1.4.1), and pandas (v1.0.1)
375 data analysis libraries. Data from biological replicates was combined and fit with a three-
376 parameter logistic model. For FRNT50's, values were simultaneously calculated for individual
377 biological replicates and patients for whom individual replicate FRNT50 values differed by more
378 than 4-fold were excluded from further analysis. Final FRNT50 values below the limit of
379 detection (1:20) were set to 1:19. Final EC₅₀ values below the limit of detection (1:1600 for
380 vaccine cohort, 1:200 for natural infection cohort) were set to 1:1599 for the vaccine cohort and

381 1:199 for the natural infection cohort. EC50 and FRNT50 curves were plotted using python with
382 the Matplotlib (v3.1.3) data visualization library.

383

384 **Statistical analysis**

385 Aggregated EC50 and FRNT50 values were analyzed in Graphpad Prism (v9.0.2). EC50 and
386 FRNT50 data were log transformed and one-way ANOVA using the Šidák multiple comparison
387 correction was used for columnated data while two-way ANOVA using the Šidák multiple
388 comparison correction was used for grouped data. The reported statistical methods are indicated
389 in the relevant figure legends. Comparison of fold reduction and 95% confidence intervals for
390 EC50 and FRNT50 were generated using one-way ANOVA. Patient samples with missing data
391 points or demographic information were excluded from individual analyses which utilized those
392 values.

393

394

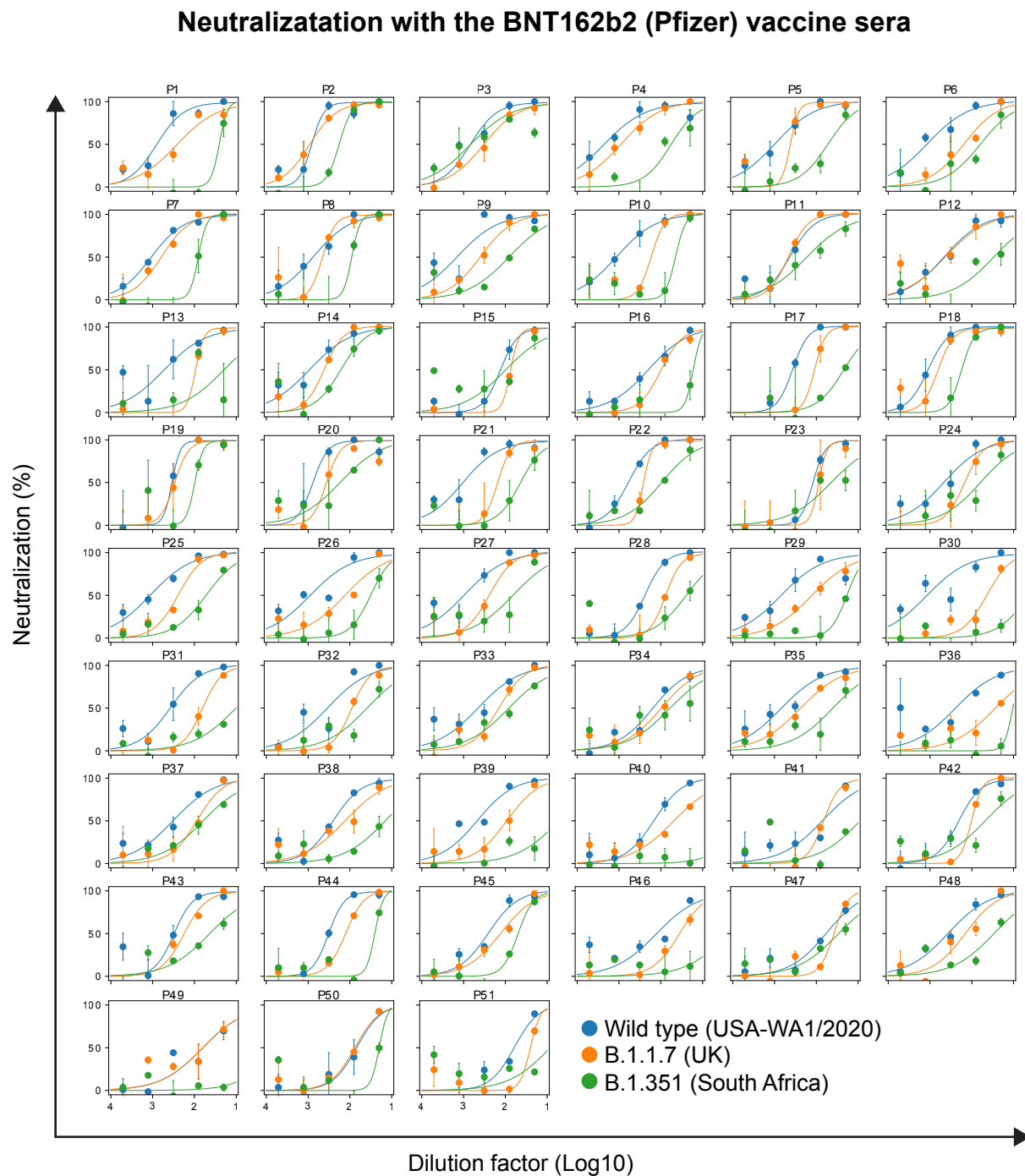
395

396 **Table S1.** List of mutations in B.1.1.7 and B.1.351 SARS-CoV-2 clinical isolates*

Lineage	GISAI Clade	GISAI ID	Spike mutations (RBD highlighted)	Non-Spike mutations
B.1.1.7	GR	EPI_ISL_683466	H69del, V70del, Y145del, N501Y , A570D, D614G, P681H, T716I, S982A, D1118H	N D3L, N G204R, N R203K, N S235F, NS8 Q27stop, NS8 R52I, NS8 Y73C, NSP3 A890D, NSP3 A1305V, NSP3 I1412T, NSP3 T183I, NSP6 F108del, NSP6 G107del, NSP6 S106del, NSP12 P323L, NSP13 K460R, NSP14 E347G
B.1.351	GH	EPI_ISL_678570	D80A, D215G, L242del, A243del, L244del, K417N , E484K , N501Y , D614G, A701V	E P71L, N T205I, NS3 Q57H, NS3 S171L, NSP2 T85I, NSP3 K837N, NSP5 K90R, NSP6 F108del, NSP6 G107del, NSP6 S106del, NSP12 P323L

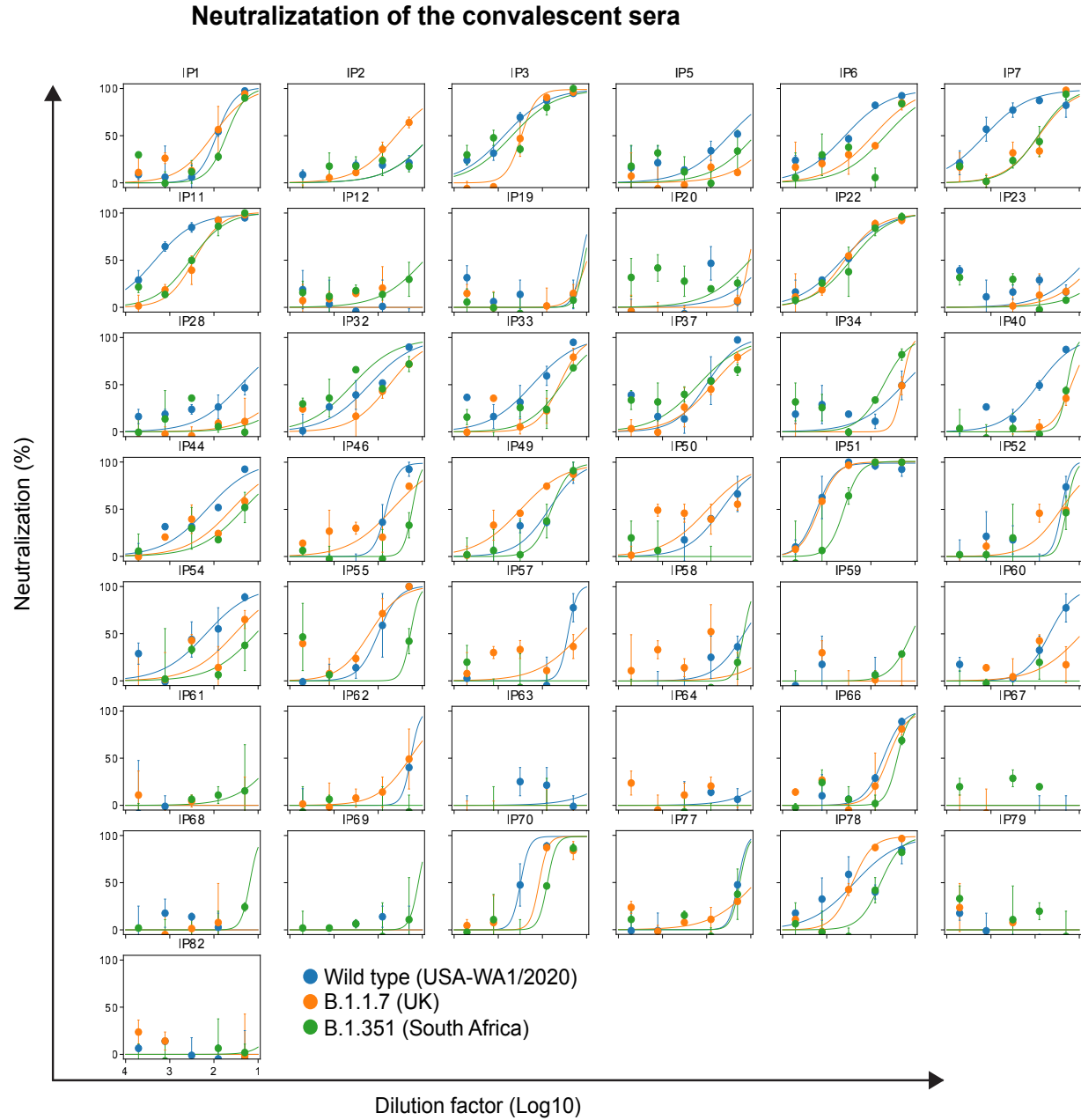
397 *Obtained from BEI Resources

398



399

400 **Figure S1.** Neutralization curves of serum (n = 51) against the different strains of SARS-CoV-2
401 are shown. Serum was collected two weeks after the second dose of the BNT162b2
402 vaccine. Error bars represent SEM of biological replicates.



403

404 **Figure S2.** Neutralization plots of convalescent sera (n = 44) against the different strains of

405 SARS-CoV-2 are shown. Error bars represent SEM of biological replicates.

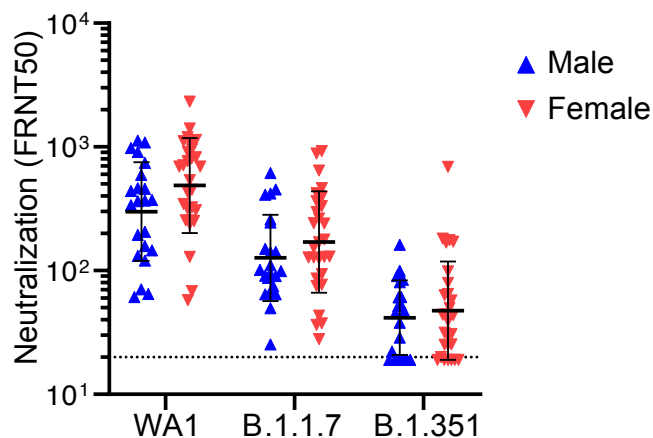
406

407

408

409

BNT162b2 vaccine- sex correlations



410

411 **Figure S3.** Comparison of vaccine sera neutralization titers (NT50) of the different SARS-CoV-

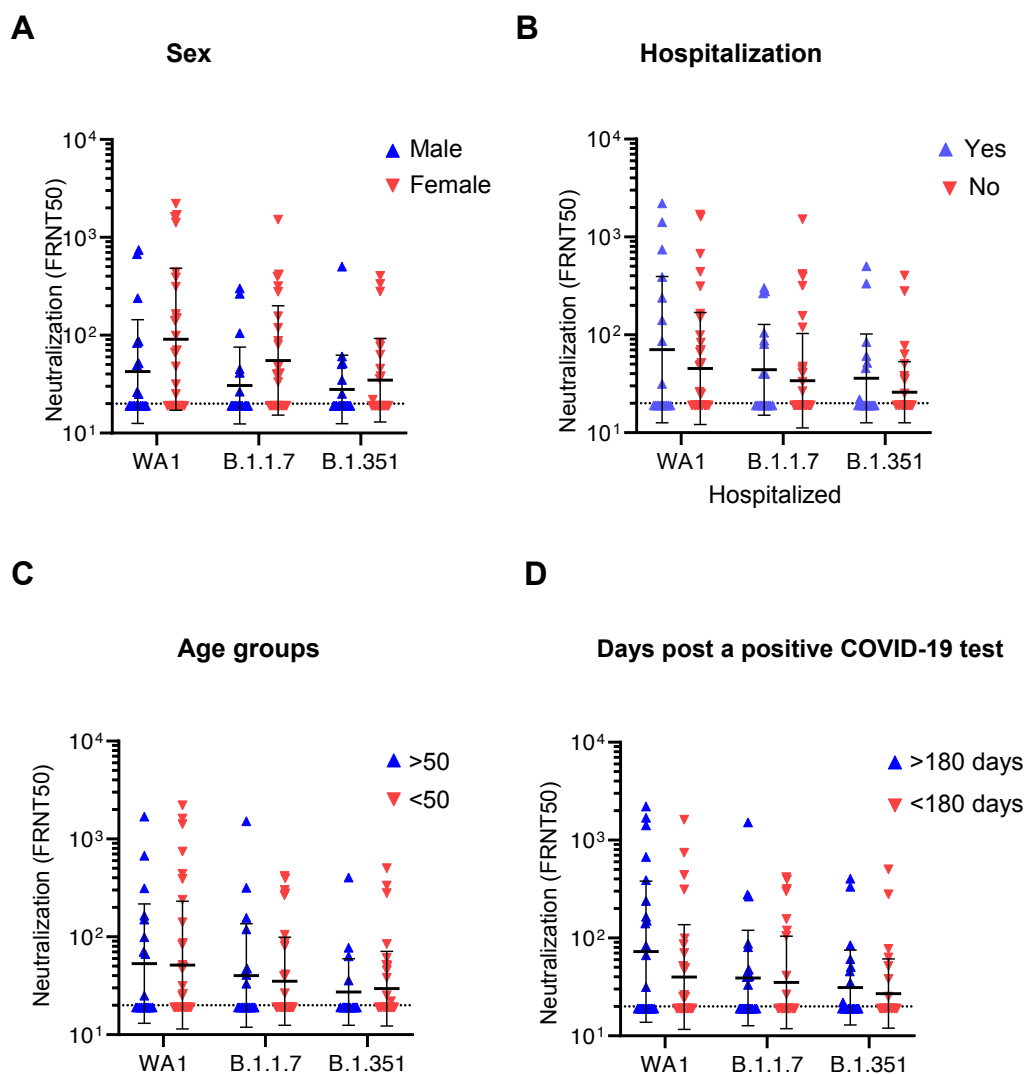
412 2 strains with sex. There is no significant correlation between gender and NT50 among vaccinees.

413 Statistical comparison was performed using a two-way ANOVA with the Šidák multiple

414 comparison correction. There is no significance correlation between vaccine serum neutralization

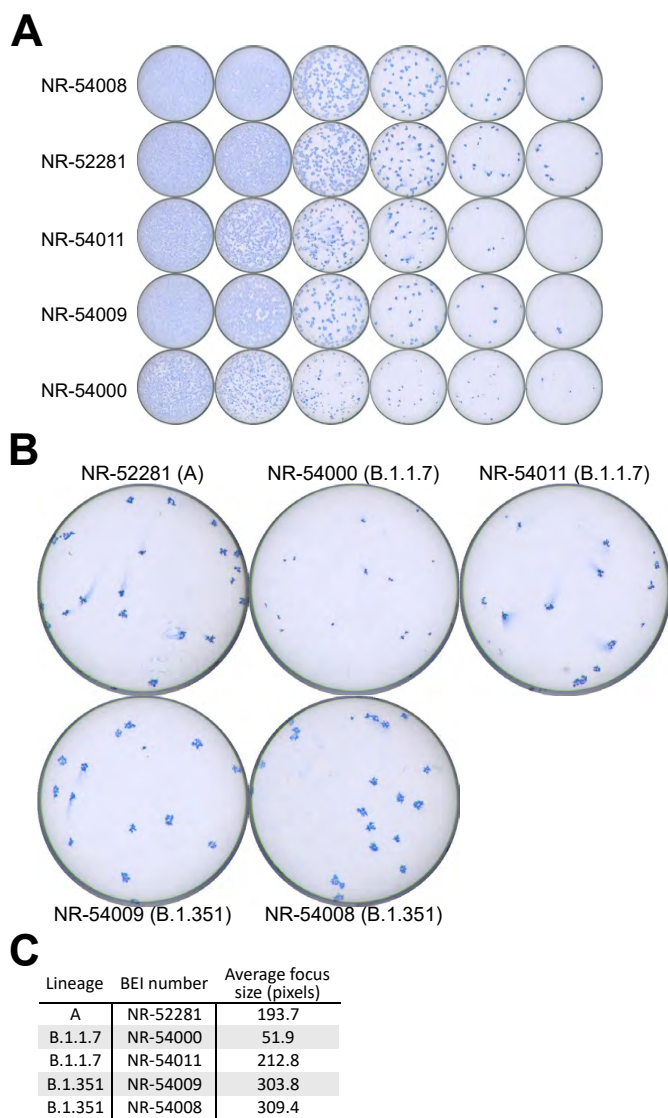
415 titers with sex.

Natural infection correlates



416

417 **Figure S4.** Correlates of selected demographic and clinical factors with neutralization in the
418 COVID-19 convalescent cohort. A-C) Correlation of convalescent neutralization titers with sex
419 (A), hospitalization versus ambulatory care (B), and age of COVID-19 patients (C). Statistical
420 comparisons were performed using a two-way ANOVA with the Šidák multiple comparison
421 correction. There is no significance correlation between convalescent neutralization titers and
422 sex, hospitalization, age or days after a positive COVID-19 test.



423

424 **Figure S5.** Focus assay well images showing an example of the utilized titration curves for the
425 clinical isolates tested during for assay development (A). Increased resolution of wells with
426 individual foci (B). Average focus size for each isolate (C). Individual focus sizes were measured
427 manually using ImageJ using the images indicated in (B). The average size indicates the mean
428 number of pixels across all foci in each image, excluding those contacting the edge of the well.

429

430 **References**

431

432 1. Holshue ML, DeBolt C, Lindquist S, et al. First Case of 2019 Novel Coronavirus in the United
433 States. *New England Journal of Medicine* 2020;382(10):929-936. DOI:
434 [10.1056/nejmoa2001191](https://doi.org/10.1056/nejmoa2001191).

435 2. Bates TA, Weinstein JB, Farley S, Leier HC, Messer WB, Tafesse FG. Cross-reactivity of
436 SARS-CoV structural protein antibodies against SARS-CoV-2. *Cell Reports*
437 2021;108737. DOI: [10.1016/j.celrep.2021.108737](https://doi.org/10.1016/j.celrep.2021.108737).

438

439

440